Integrative Biosciences 9: 65-73, 2005

Integrative
Biosciences
http://www.ibiosci.or.kr

Cytochemical Localization of Nuclear Actin of Sperm and Spermatids in *Urechis unicinctus*

Kil-Sang Shin, Ho-Jin Kim, Hyuk-Jae Kwon and Wan-Jong Kim*

Department of Life Science, College of Natural Sciences, Soonchunhyang University, Asan 336-745, Korea

Abstract: In this study, we found that sperm ball of *Urechis unicinctus* consisted of a somatic cell and spermatogenic cells. After separation from the sperm ball, individual spermatid floated freely in the coelomic fluid and differentiated into a mature sperm. Because of many nuclear vacuoles, spermatid nucleus was observed to be heterogeneous. Later, the spermatid nucleus condensed into the homogeneous round nucleus of the mature sperm. Perinuclear microtubules could be seen but did not seem to be organized into manchette microtubules. To understand the nature of nuclear condensation during spermiogenesis, the sperm and spermatids (spermiogenic cells) were treated with FITC-phalloidin, or anti-actin-FITC, or labeled with anti-actin immunogold particles (AAIP; 10 nm) followed by transmission electron microscopy or confocal laser scanning microscopy. The anti-actin-FITC and FITC-phalloidin reactions occurred distinctly in the nuclei of both spermiogenic cells. FITC-phalloidin reacted more intensely with acrosomes. The AAIP were incorporated mainly into nuclei of both cells sometimes showing local distribution in the nucleus. Nuclear vacuoles of spermatids disappeared progressively with condensation of the nucleus, as the number of incorporated AAIP/μm^2 increased. These results suggest that nuclear actin microfilaments might be closely related to nuclear condensation.

Key words: *Urechis unicinctus,* spermiogenic cells, actin, phalloidin, immunogold

Urechis unicinctus (spoon worm; innkeeper) is a marine invertebrate. During the breeding season, body cavity is filled with coelomic fluid containing coelomocytes, mature sperm, spermatids, and sperm balls composed of a somatic cell and many spermatogenic cells (Shin, 1988). All of these components are individual single cells floating freely in the coelomic fluids. The sperm and spermatids arise from sperm ball, and when they reach the spermatid stage, separate from the sperm ball through cytoplasmic bridge, similar to exocytotic vesicles of secretory cells. The nuclear matrices of spermatids contain many nuclear vacuoles, while a few nuclear vacuole are seen in the nuclear matrices of mature sperm. Nuclear condensation seem to occur with progressive disappearance of the nuclear vacuoles. The sperm nucleus is reduced in volume by a half of spermatid nucleus.

The condensation of spermatid nucleus occurring in the coelomic fluids is not clearly understood. Nuclear condensation of male generative cells can occur either by extrinsic factors such as perinuclear microtubules, or by intrinsic factors such as histone-like basic proteins. Recently, it was reported that structural correlations between extrinsic actin microfilaments derived from Sertoli cell and manchette microtubules of sperm play a role in condensation and shaping of spermatids in mice and rats (Kierszenbaum et al., 2003). In *U. unicinctus*, perinuclear microtubules are observed, but are not organized to form a manchette, and histone-like basic proteins have not been analysed.

Since nuclear matrices contain actin microfilaments with a set of other proteins (Kramer and Krawetz, 1996), nuclear actin microfilaments may guide the individual nucleus through gradual disappearance of nuclear vacuoles to the condensation of mature sperm. With this consideration, spermiogenic cells of *U. unicinctus* were treated with anti-actin-FITC, anti-actin-immunogold particles (AAIP; 10 nm) and FITC-phalloidin, in order to know the roles of actin microfilaments in condensation of nucleus. This is also because of known function of actin microfilaments in cell shaping and maintaining nuclear shape (Cooper, 1991; Soyer-Gobillard et al., 1996). Confocal laser scanning microscopy (CLSM) revealed that nuclei of spermiogenic cells positively reacted to FITC-phalloidin and anti-actin-

*To whom correspondence should be addressed.
Tel: 82-41-530-1251, Fax: 82-41-530-1256
E-mail: wjkim56@sch.ac.kr

FITC, respectively. The incorporation of AAIP (10 nm)/ μm^2 tended to increase in number as spermiogenesis proceeded, while the nuclear vacuoles of spermatids disappeared gradually from the nuclear matrices. From this, it was suggested that actin-based nuclear condensation could occur in the *U. unicinctus* spermatids.

With FITC-phalloidin treatment, on the other hand, the acrosomal materials were most reactive and were not expended, when egg-vitelline layer was removed prior to insemination. The acrosomal materials may have a role to facilitate adhesion of sperm on the vitelline layer.

MATERIALS AND METHODS

Electron microscopy

Spermiogenic cells of *U. unicinctus* were prepared from coelomic fluids obtained by making an incision in the vertical body wall. Low speed centrifugation (~300 rpm) of the coelomic fluid separated approximately the upper supernatant of mature sperm and lower supernatant of spermatids including sperm balls from the precipitate containing coelomocytes.

For artificial insemination, mature eggs were obtained form the upper layer of ovary, and washed several times in 0.45 μm millipore filtered natural sea water (18-22‰). The sperm and eggs at ratio of 400:1 were fertilized artificially in natural sea water for 3-5 min. The methods of artificial insemination followed by cytological observation often revealed configurations that sperm remained on egg-vitelline layer, although the acrosomal materials seemed to be expended. To visualize actual role of the acrosomal materials, the vitelline layer was removed from the egg by treatment with 0.1% Triton X-100 for 2 h, and the eggs were used in fertilization.

The spermiogenic cells and fertilized eggs were used for EM and immunolabeling preparations. The materials for EM observation were prefixed in 0.1M phosphate buffered 4% formaldehyde containing 0.5% glutaraldehyde for 1 h at 4°C, and fixed in 0.1M phosphate buffered 2.5% glutaraldehyde for 2 h. The materials were washed in 0.2M phosphate buffer, and postfixed in 1% OsO_4 for 2 h. After washing in distilled water, the materials were dehydrated in series of graded concentrations of ethanol and prophylene oxide, and embedded in Araldite mixture. The blocks were incubated for overnight at 40°C, 60°C, and 65°C, respectively. Centrifugation was needed once for all prior to prefixation, because of the fast precipitation of the materials in each step. Blocks were sectioned on OM-2 Reichert microtome. Sections were contrasted in saturated aqua solution of uranyl acetate and lead citrate, examined on JEOL 1010B electron microscope.

Immunofluorescence methods and CLSM

FITC-phalloidin was dissolved in methanol to make 3.3 μM FITC-phalloidin solution. This solution was diluted 50-100 times with 0.1M Tris buffer just before use. The spermiogenic cells were smeared gently on cover glasses which had been previously treated with 10% aqua solution of Poly-L-Lysine. The materials were stained for 1 h in moisture chamber at 4°C, and the excess FITC-phalloidin solutions were washed off with the same buffer. The cover glasses were mounted on slide glass with Gel mount.

The commercial amoeba monoclonal anti-actin conjugate was diluted with 0.1M Tris buffer (1:1,000). For anti-actin-FITC reactions, the same method as the above excluding the staining time (5-6 h) was applied. The preparations were observed by CLSM using 15 mW Krypton/Argon laser power (15-30%).

Since the FITC-phalloidin and anti-actin-FITC conjugate showed weak reaction to flagella, it was often obligatory to view the whole sperm structures under CLSM. The spermiogenic cells were treated in anti-α-tubulin solution to imprint α-tubulin. The antibody solutions were diluted 1,000× with 0.1M Tris buffer. The antibodies were then marked with the anti-mouse IgG-FITC conjugates diluted in the same buffer. The immunostaining methods of multisteps, FITC-phalloidin and anti-actin-FITC followed by anti-α-tubulin, were more effective to observe the imprinted immunofluorescences on the whole spermiogenic cells.

Anti-actin immunogold labeling and transmission electron microscopy

The AAIP (10 nm) labeling and electron microscopy used in this work were in principle followed De May's "postembedding methods." (De May, 1983). For the invertebrate materials, some details were modified as described below. The materials of immunogold labeling groups were prefixed in 0.1M phosphate buffered 4% formaldehyde with 0.5% glutaraldehyde containing 0.1% $CaCl_2$ (Gould-Somero and Holland, 1975; Elinson and Manes, 1978). For further treatments, the same methods as described in the above section were applied and then AAIP were labeled as follows. The 70-80 nm ultrathin sections were gathered on nickel grids, etched in 10% H_2O_2 for 3-5 min. Thereafter, the sample grids were treated with gelatin, glycine solution and 1% BSA solution respectively, rinsed 3 times in phosphate buffered saline solution. The samples were incubated for 4-6 h with amoeba monoclonal anti-actin (mouse-IgG isotype) (1:100 to 200) in moisture chamber at 4°C. The AAIP conjugated goat anti-mouse-actin which was diluted 200× was used to mark the primary antibody. The samples were then fixed in 1% glutaraldehyde and 0.2% OsO_4 for 1 min. The sections were stained in

saturated aqua solution of uranyl acetate and lead citrate, and observed on JEOL 1010B transmission electron microscope.

RESULTS

Spermiogenic cells

Two kinds of spermiogenic cells could be observed from preparation of coelomic fluids. One kind of cells was sperm with small (2 μm) diameter that has homogeneous nuclear matrices (Fig. 1A), and the other was spermatid with larger (3-4 μm) diameter that has heterogeneous nuclear matrices (Fig. 1B). It was revealed the former type was primarily involved in artificial insemination, associated closely with the egg-vitelline layer. The latter, spermatids, were enclosed with undulating cell membrane, contained still numerous nuclear vacuoles and much of cytoplasm at level of posterior nuclear fossa.

Spermatids have been often observed in close connection by narrow cytoplasmic bridge with sperm balls composed of spermatogenic cells and a somatic cell. The configuration of cytoplasmic bridges appear to be similar to exocytotic vesicle of secretory cells. Cytologically, it seemed that the spermatids were separated from the sperm ball into the body cavity. The somatic cells composed of sperm ball appeared only during the breeding season, and were large in size (~50 μm in diameter) with abundant cytoplasm and a prominent nucleus. After separation from sperm ball, floating freely in the coelomic fluids, the spermatids differentiated further into mature sperm. Various intermediate stages of developing spermatids could be observed with different grades of nuclear condensation and sizes.

Excluding the nucleus, sperm organelles were similar to those of spermatids in their sizes and shapes. The acrosome was discoid in shape, located in anteriorly invaginated site of nuclear envelope and bipartite with outer and inner regions. The outer circumferential region was electron dense contrasting with the inner region that was a less electron dense. Both regions of acrosome were enclosed with membrane. The outer membrane protruded forwardly and the inner acrosomal region was surrounded lengthwise by slender subacrosomal fossa whose apex was concave and more or less widened as a whole. Between the subacrosomal fossa and anteriorly-invaginated nuclear envelope was perinuclear fossa, which was convex in shape. Mitochondria seemed arranged as a circular band along the outer margin of the posterior nuclear fossa. Cell membrane was undulated and slightly widened at the level of posterior nuclear fossa, so that much of the cytoplasm was accumulated in the region. The proximal centriole of spermatids appeared to be connected with fractional extensions of nuclear envelope, whereas this was disconnected in case of sperm. At fertilization, acrosomal material became loose to form fine particles which coated the surface of developing acrosomal process (0.5 μm in length) and were simultaneously scattered and dispersed toward the egg-vitelline layer (Fig. 1C). On fine structure, seemed that the acrosomal materials were expended on the materials composing the vitelline layer. When the vitelline layer was removed from egg prior to fertilization, the acrosomal materials did not loosen, but remained structurally intact, making a close contact with the oolemma (Fig. 1D).

The CLSM and the labeling of AAIP

The acrosomal materials of spermiogenic cells were intensely stained with FITC-phalloidin fluorescence, while the nuclear matrices exhibited moderate immunofluorescence (Fig. 2A). When the spermiogenic cells were stained with anti-actin-FITC conjugates, their nuclei reacted positively with similar fluorescence. However, acrosomes of both sperm and spermatids reacted negatively. Flagella were negative for both immunofluorescence stains (Fig. 2B). When the samples were treated serially with the two kinds of immunofluorescence dyes, followed by anti-α-tubulin-FITC conjugate, then green immunofluorescence could be observed on the whole patterned structures of the spermiogenic cells (Figs. 2C and D).

The immunogold labelings were varied with subcellular compartments of the spermiogenic cell. The incorporated AAIPs were not detected on cytoplasm and flagellum, and a few number of AAIP/μm^2 were observed to be incorporated into subacrosomal and perinuclear fossa. The AAIP-incorporation into the perinuclear fossa were varied among spermiogenic cells. In some, a few AAIP or no AAIP were detected. The incorporated AAIP were detected in the subacrosomal fossa in most cases. AAIP was incorporated primarily into the nuclear matrices. The number of incorporated AAIP/μm^2 varied slightly among nuclei of spermiogenic cells. The nucleus of mature sperm showed an increasing number of incorporated AAIP/μm^2 (Fig. 3A and B), while a decreasing number was observed with the spermatid nucleus (Figs. 3C and D). The number of incorporated AAIP/μm^2 tended to vary linearly with the developmental stages (Fig. 4), and in turn, the aspects of AAIP-incorporation were often contrasted with progressive disappearance of nuclear vacuoles from the nucleus. Where many nuclear vacuoles are scattered, less number of AAIP/μm^2 were incorporated. The local concentration of AAIP in a nuclear region increased inversely with appearance of nuclear vacuoles. Since the nuclear condensation proceeded until spermatid nucleus reduced in volume by a half, a tendency that the AAIP-incorporations were inversely proportional to appearance of nuclear vacuoles have been

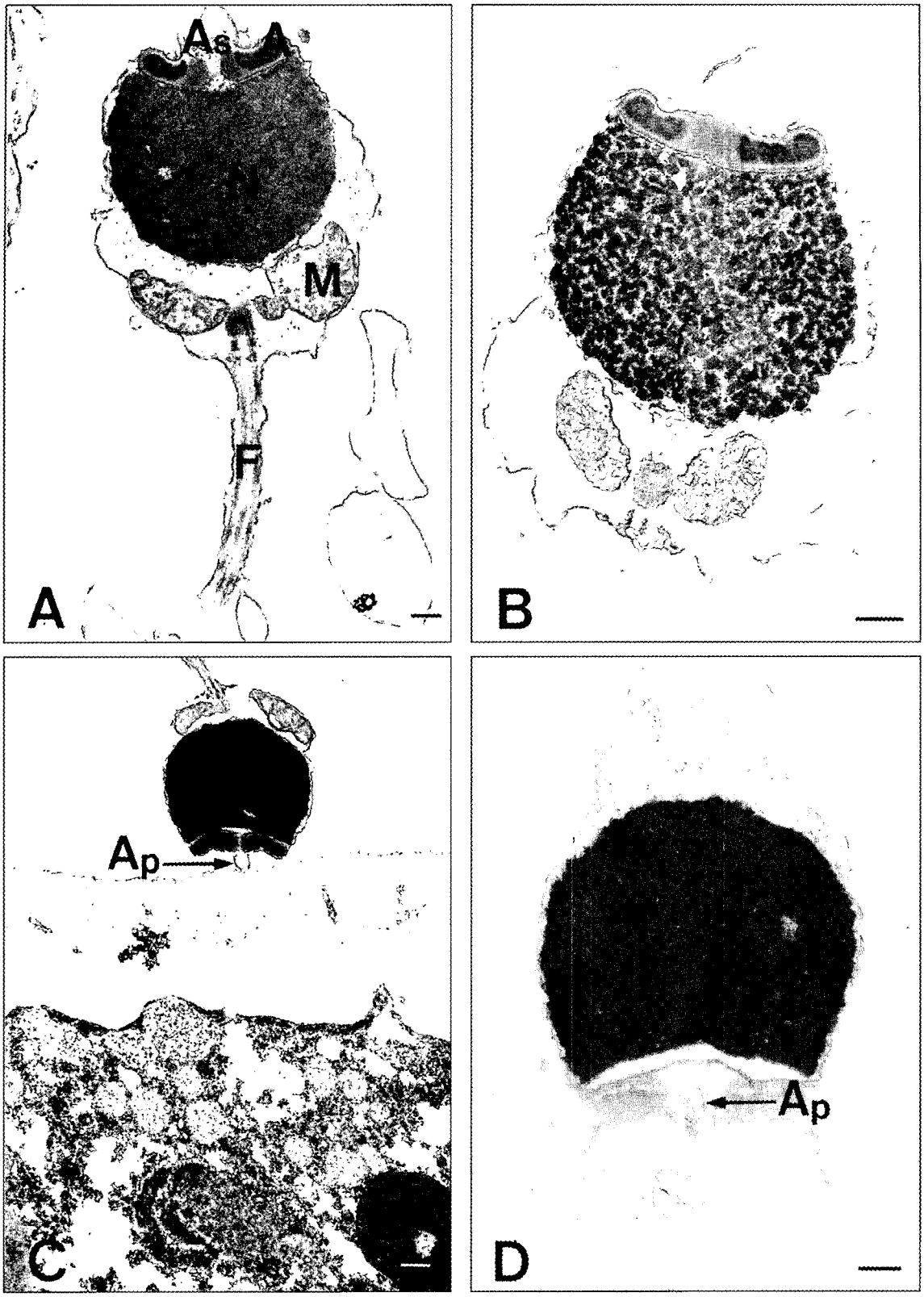

Fig. 1. A, Electron micrograph of a mature spermatozoon with homogeneous nuclear matrices and acrosome. B, A spermatid with granular nuclear matrices with its nuclear vacuoles. C, Artificial inseminated *Urechis* sperm and egg. The sperm contacts with the surface coat of the egg, but there is no acrosomal process to be seen in this median section. D, A spermatozoon has penetrated the surface coat of the egg and contacts with egg cytoplasm. A: Acrosome, Ap: Acrosomal process, As: Acrosomal space, F: Flagellum, M: Mitochondrion, N: Nucleus, Scale bars = 200 nm.

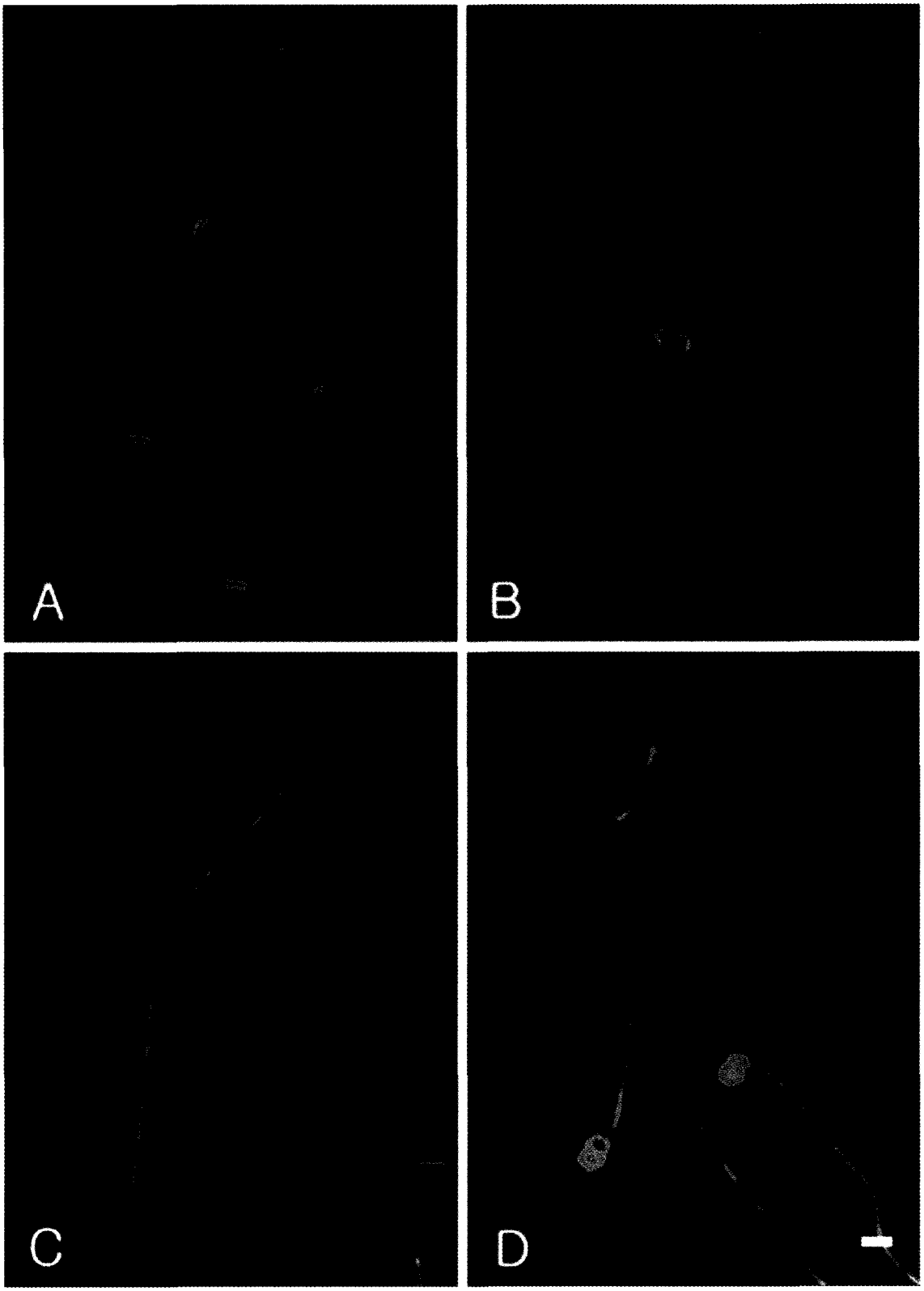

Fig. 2. A, Confocal laser scanning microscopy (CLSM) of the anti-actin labeled and FITC-phalloidin stained sperm and spermatids. B, The CLSM of anti-actin and anti-actin-FITC labeled sperm and spermatids. C. The CLSM of anti-tubulin and anti-tubulin-FITC labeled sperm and spermatids. D, The CLSM of triple fluorescence stained sperm and spermatids. Scale bar = 5 μm.

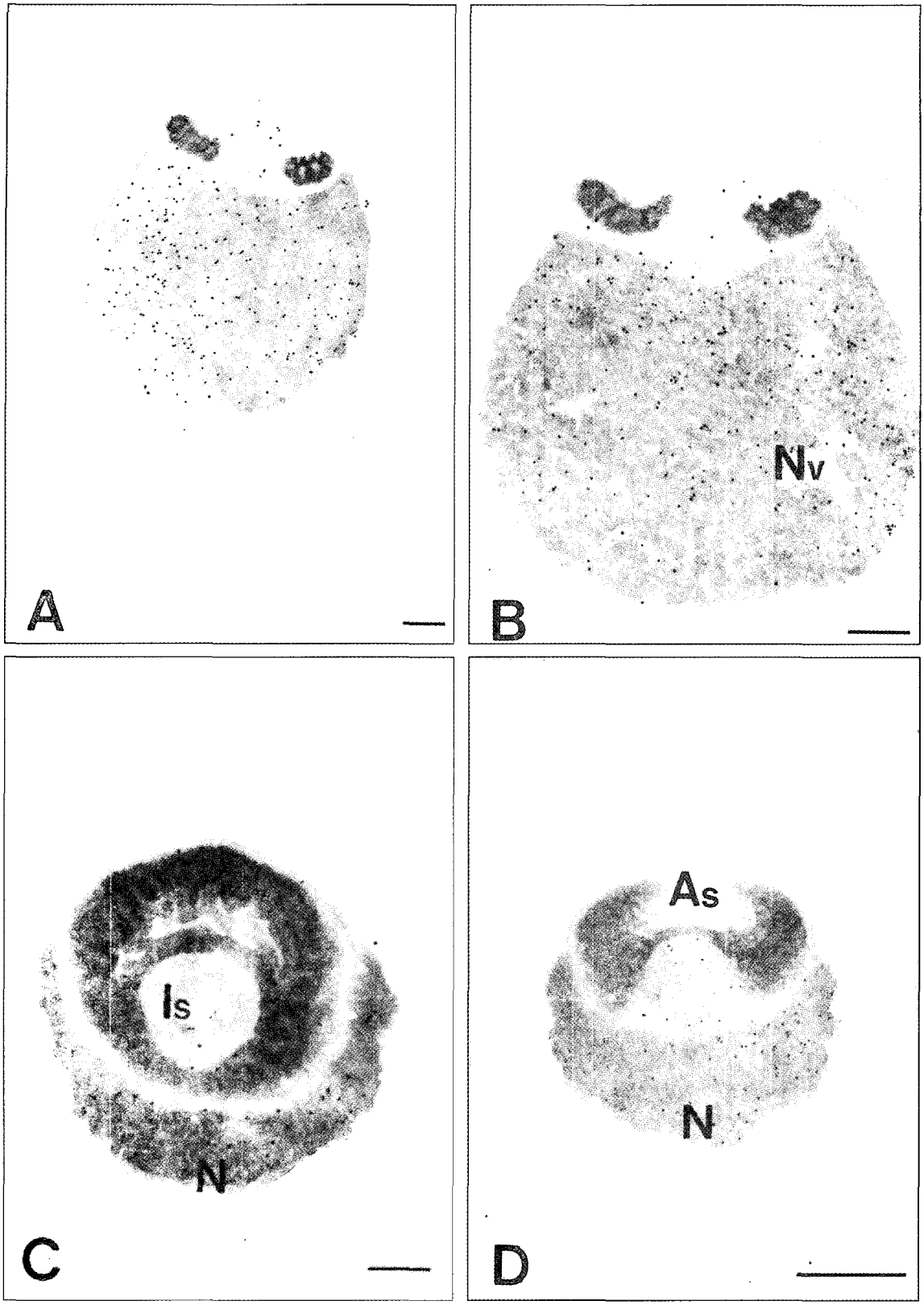

Fig. 3. A, Anti-actin-gold (10 nm) labeled nuclear matrices of a spermatozoon. Since the anti-actin binds to G-actin, the G-actin is a component of the nuclear matrices. B, Anti-actin-gold (10 nm) labeled nuclear matrices of the spermatid. C, The gradient acrosome can be seen in this cross section through the acrosome of sperm. D, A slightly oblique section through the acrosome of spermatid. As: Acrosomal space, Is: Inner space, N: Nucleus, Nv: Nuclear vacuole. Scale bars = 200 nm.

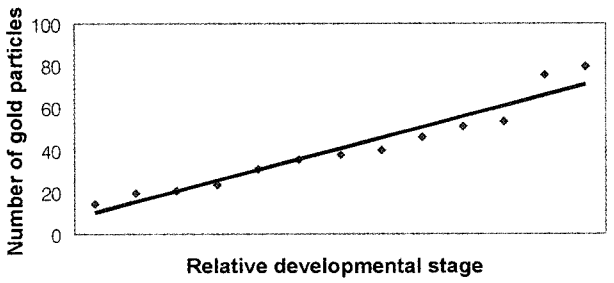

Fig. 4. Labeled immunogold particles per μm^2 in developing spermiogenic cells.

observed to occur during the spermiogenesis. And since the small compacted nucleus of mature sperm showed the most incorporation of AAIP, developmental stage could be distinguished by the number of incorporated AAIP/μm^2.

DISCUSSION

Spermiogenic cells

Coelomic fluid of male *U. unicinctus* was filled with four kinds of cells, and it was technically difficult to distinguish spermatid from the sperm in the preparations of coelomic fluids. Therefore, the term "spermiogenic cell" was used collectively to refer the individual sperm inclusive of spermatids proceeding spermiogenesis. The term "spermiogenic cell" has embraced the coelomic mature sperm which were not yet accumulated in distinct testes for discharge, but excluded the cells attaching to sperm ball which did not enter the stage of spermiogenesis.

In view of immunochemical and immunofluorescence observations, it seemed that one of main events of *U. unicinctus* spermiogenesis was nuclear condensation of the spermiogenic cells. The nuclear vacuoles of the spermatids disappeared progressively reducing the volume to 43% on average. It was known that condensation of nuclear volume or shaping of sperm was based on either by manchette microtubules (McIntosh and Porter, 1967) or substitution of histone with protamine, a histone-like basic protein (Hecht et al., 1986) or hyperacetylation of histone (Oliva et al., 1987). The manchette microtubules consist of interconnections of extrinsic or perinuclear microtubules surrounding spermatid nucleus (Wilkinson et al., 1974; Medina et al., 1988). Microtubules were found around nucleus in *U. unicinctus* sperm, but were scattered in perinuclear cytoplasm and not organized to form functional manchette (Shin, 1998). The scattered microtublules seemed not to be an intermediate transient form processing assembly or disassembly of a manchette (Yoshida et al., 1994). In most known cases, the role of manchette microtubules is to extent elongation of sperm nucleus, but the nucleus of *U. unicinctus* is round in shape with anterior invagination of nuclear envelope. Ectoplasmic F-actin of Sertoli cell in mouse and rat coordinated with perinuclear microtubules and the structural complex may apply forces steering the extent elongation of the spermatid nucleus (Kierszenbaum et al., 2003). It seemed not to enable to be out-source of actin microfilaments because the spermiogenic cells of *U. unicinctus* were single free cells. In cases of somatic cells, perinuclear or cytoplasmic actin microfilaments are known to play a direct role in cell shaping and maintaining nuclear shape (Cooper, 1991; Soyer-Gobillard et al., 1996). It was suggested that nuclear condensation of the spermiogenic cells in *U. unicinctus* was caused by intranuclear, not by perinuclear actin microfilaments as known in the somatic cells. In addition, histone-like basic protein involving nuclear condensation was not yet known in *U. unicinctus*.

Little is known about the direct role of intranuclear actin microfilaments in condensation of spermatid nucleus and nuclear shaping. However, the results of this work might indicate that actin microfilaments-based nuclear shaping occurred in the *U. unicinctus* spermiogenic cells. This consideration is based on differential reactions of the spermiogenic cells to the immunofluorescence staining and amoeba monoclonal anti-actin specific incorporation of AAIP/μm^2. The nuclei of spermiogenic cells showed positive reactions to both FITC-phalloidin and anti-actin-FITC, implicating that the nuclear matrices contained both actin polymer and monomer. The immunofluorescence staining revealed similar tendency with incorporations of AAIP. The numbers of incorporated AAIP/μm^2 varied with developmental stages and degree of nuclear condensation. The nuclear condensations were accompanied by progressive disappearance of the nuclear vacuoles. As a whole, the number of incorporated AAIP/μm^2 increased as directly as developmental progress. In turn, the number of incorporated AAIP/μm^2 increased inversely with appearance of nuclear vacuoles, while the nuclear matrices contained still less number of nuclear vacuoles. The immunogold labeling often showed local concentration or regional distribution within a nucleus. Regional or local reduction of nuclear volume could occur within a nucleus. Finally, as the number of incorporated AAIP/μm^2 further increase, the nuclear vacuoles were difficult to be seen and the nucleus became more compact reaching spherical configuration. The stage distributions of the spermiogenic cells could be expressed with respect to the number of incorporated AAIP/μm^2 coinciding with decrease of the nuclear vacuoles. Since actin assembly and disassembly are interrelated, it is suggested that the increased number of AAIP/μm^2 may be correlated with switching on disassembly of F-actin by increased availability of actin monomer to react with the AAIP. The actin microfilaments can be released from reorganization of genome for protamine replacement (Kramer and Krawetz, 1996).

However, phase-change of actin microfilaments alone

(Soyer-Gobillard et al., 1996; Holly and Blumer, 1999) is not enough to change cell shaping or maintaining nuclear shape. Because of rigidity, membrane components alone can not be a factor to change cellular volume (Egile et al., 1999; Mallavarapu and Mitchison, 1999). Coordinate effects between the membrane and vectorial energy derived from the assembly or disassembly of the actin-based microfilaments would be required for the cell to change the shape (Verkovsky and Borisy, 1993), of which activities necessitates a set of actin binding proteins. The coordinate effects inevitably enable local retraction or extension of membrane in course of cell shaping (Hoey and Gavin, 1992). The local concentration of AAIP/μm^2 coinciding association with local disappearance of nuclear vacuoles may implied that a local condensation can be occurred in *U. unicinctus* spermiogenic cells.

Acrosome

The FITC-Phalloidin reacted intensely to acrosome, while the anti-actin-FITC reactions could not be observed in the acrosome of *U. unicinctus* spermiogenic cells. Gould-Somero and Holland (1975) suggested that the acrosomal material might be an adhesive in *U. caupo*. Since FITC-phalloidin bound to actin filaments much more tightly than to actin monomer and shifted the equlibrium between filaments and monomer towards filaments (Faulstich et al., 1977; Estes et al., 1981), it was suggested that the acrosome could encompassed F-actin. Similar results were reported in sand dollars that the acrosomal materials were composed of microfilamentous material and had a role to play in bindin (Summers and Hylander, 1974). The acrosomal materials of U. unicinctus appeared equivalent to bindin of other marine invertebrates. Bindin has two roles to play in fertilization, facilitating sperm-egg adhesion between reacted sperm to the egg membrane and inducing of acrosomal reaction of the 2nd binding (Glabe and Vacquier, 1978; Inoue and Tilney, 1982). But, in detail, the bindin of *U. unicinctus* revealed some other characteristics during artificial insemination. When egg-vitelline was removed and these eggs were fertilized, the bindin materials were not expended, but remained intact until sperm contacted closely on the oolemma, otherwise, the materials of bindin were expended and dispersed as a fine particles on acrosomal process and egg-vitelline layer. Since the fine particles were derived from the bindin and covered developing acrosomal process, it is suggested the bindin-material plays a role in protecting the acrosomal process.

Acrosomal process

Although only a few numbers of AAIP/μm^2 were incorporated into the subacrosomal fossa, they were observed in most cases of examinations, while the number of incorporated AAIP/μm^2 into the perinuclear fossa was varied among spermiogenic cells, sometimes no AAIP and in other times a few AAIP were observed. It was reported that in acrosomal process, actomere could be centrifugally polymerized and self-assembled from the stored G-actin by its local concentration in the acrosome (Fath and Burgess, 1995). However, the localizations of G-actin in a sperm were different from reported species. These are, for instances, anterior nuclear fossa (*pupuratus*: Tilney, 1978; Verkovsky and Borisy, 1993), perinucelar fossa (bull, rabbit, hamster: Flaherty et al., 1988), subacrosomal space (mouse: Prigent and Dadoune, 1993), subacrosomal bulges (rabbit: Fouquet and Kann, 1992) and fibrous sheath (human: Flaherty et al., 1988; Escalier et al., 1997). The localization of G-actin is species-specific (Fouquet and Kann, 1992). In *U. unicinctus* sperm, it seemed that the perinuclear fossa was the principal site of G-actin localization, which could diffuse into the subacrosomal fossa in the time period of actomere formation. When the G-actin was exhausted by the diffusion from perinuclear fossa, no AAIP could be incorporated into the perinuclear fossa.

REFERENCES

Cooper JA (1991) The role of actin polymerization in cell motility. *Annu Rev Physiol* 53: 585-605.

De May JR (1983) The preparation of immunoglobulin gold conjugated (IGS reagents) and their use as markers of light and electron microscopic immunocytochemistry. In: Cuello AC (ed), Immunohistochemistry, Wiley, New York, pp 347-372.

Egile C, Loisel TP, Laurent V, Li R, Pantaloni D, Sansonetti PJ, and Carlier MF (1999) Activation of the CDC42 effector N-WASP by the *Shigella flexneri* IcsA protein promotes actin nucleation by Arp2/3 complex and bacterial actin-based motility. *J Cell Biol* 146: 1319-1332.

Elinson RP and Manes ME (1978) Morphology of the site of sperm entry on the frog egg. *Dev Biol* 63: 67-75.

Escalier D, Gallo JM, and Schrevel J (1997) Immunochemical characterization of a human sperm fibrous sheath protein, its developmental expression pattern, and morphogenetic relationships with actin. *J Histochem Cytochem* 45: 909-922.

Estes JE, Selden LA, and Gershman LC (1981) Mechanism of action of phalloidin on the polymerization of muscle actin. *Biochemistry* 20: 708-712.

Fath KR and Burgess DR (1995) Microvillus assembly. Not actin alone. *Curr Biol* 5: 591-593.

Faulstich H, Schafer AJ, and Weckauf M (1977) The dissociation of the phalloidin-actin complex. *Hoppe-Seyler's Z Physiol Chem* 358: 181-184.

Flaherty SP, Winfrey VP, and Olson GE (1988) Localization of actin in human, bull, rabbit, and hamster sperm by immunoelectron microscopy. *Anat Rec* 221: 599-610.

Fouquet JP and Kann ML (1992) Species-specific localization of actin in mammalian spermatozoa, fact or artifact? *Micros Res Tech* 20: 251-258.

Glabe CG and Vacquier VD (1978) Egg surface glycoprotein receptor for sea urchin sperm bindin. *Proc Natl Acad Sci USA*

75: 881-885.

Gould-Somero M and Holland L (1975) Fine structural investigation of the insemination response in *Urechis caupo*. *Dev Biol* 46: 358-369.

Hecht NB, Bower PA, Waters SH, Yelick PC, and Distel RJ (1986) Evidence for haploid expression of mouse testicular genes. *Exp Cell Res* 164: 183-190.

Hoey JG and Gavin RH (1992) Localization of actin in the *Tetrahymena* basal body-cage complex. *J Cell Sci* 103: 629-641.

Holly SP and Blumer KJ (1999) PAK-family kinases regulate cell and actin polarization throughout the cell cycle of *Saccharomyces cerevisiae*. *J Cell Biol* 147: 845-856.

Inoue S and Tilney LG (1982) Acrosomal reaction of thyone sperm. I. Changes in the sperm head visualized by high resolution video microscopy. *J Cell Biol* 93: 812-819.

Kierszenbaum AL, Rivkin E, and Tres LL (2003) Acroplaxome, an F-actin-keratin-containing plate, anchors the acrosome to the nucleus during shaping of the spermatid head. *Mol Biol Cell* 14: 4628-4640.

Kramer JA and Krawetz SA (1996) Nuclear matrix interactions within the sperm genome. *J Biol Chem* 271: 11619-11622.

Mallavarapu A and Mitchison T (1999) Regulated actin cytoskeleton assembly at filopodium tips controls their extension and retraction. *J Cell Biol* 146: 1097-1106.

McIntosh JR and Poter KR (1967) Microtubules in the spermatids of the domestic fowl. *J Cell Biol* 35: 153-173.

Medina A, Moreno FJ, and Garcia-Herdugo G (1988) Sperm tail differentiation in the nudibranch mollusc *Hypselodoris tricolor* (Gastropoda, Opisthobranchia). *Gam Res* 20: 223-232.

Oliva R, Bazett-Jones D, Mezquita C, and Dixon GH (1987) Factors affecting nucleosome disassembly by protamines in vitro. Histone hyperacetylation and chromatin structure, time dependence, and the size of the sperm nuclear proteins. *J Biol Chem* 262: 17016-17025.

Prigent Y and Dadoune JP (1993) Immunoelectron microscopic distribution of actin in the spermatids and epididymal spermatozoa of the mouse. *Acta Anat* 147: 133-139.

Shin KS (1998) The fine structure of the sperm ball and sperm of *Urechis unicinctus* and immunogold localization of α-tubulin. *Korean J Elec Micros* 28: 193-205.

Soyer-Gobillard MO, Ausseil J, and Geraud ML (1996) Nuclear and cytoplasmic actin in dinoflagellates. *Biol Cell* 87: 17-35.

Summers RG and Hylander BL (1974) An ultrastructural analysis of early fertilization in the sand dollar, *Echinarachnius parma*. *Cell Tiss Res* 150: 343-368.

Tilney LG (1978) Polymerization of actin. V. A new organelle, the actomere, that initates the assembly of actin filaments in thyone sperm. *J Cell Biol* 77: 851-864.

Verkovsky AB and Borisy GG (1993) Nonsarcomeric mode of myosin II organization in the fibroblast lamellum. *J Cell Biol* 123: 637-652.

Wilkinson RF, Stanley HP, and Bowman JT (1974) Genetic control of spermiogenesis in *Drosophila melanogaster*, the effects of abnormal cytoplasmic microtubule populations in mutant ms(3)10R and its colcemid-induced phenocopy. *J Ultrastr Res* 48: 242-258.

Yoshida T, Ioshii SO, Imanaka-Yoshida K, and Izutsu K (1994) Association of cytoplasmic dynein with manchette microtubules and spermatid nuclear envelope during spermiogenesis in rats. *J Cell Sci* 107: 625-633.

[Received March 18, 2005; accepted May 23, 2005]